CHEMISTRY OF MATERIALS

Communication

pubs.acs.org/cm

High-Mobility Bismuth-based Transparent *p*-Type Oxide from High-Throughput Material Screening

Amit Bhatia,[†,⊥] Geoffroy Hautier,[*,‡,⊥] Tan Nilgianskul,[†] Anna Miglio,[‡] Jingying Sun,[§] Hyung Joon Kim,[∥] Kee Hoon Kim,[∥] Shuo Chen,[§] Gian-Marco Rignanese,[‡] Xavier Gonze,[‡] and Jin Suntivich[*,†]

[†]Materials Science and Engineering Department, Cornell University, Ithaca, New York 14850, United States

[‡]Institute of Condensed Matter and Nanosciences, Université catholique de Louvain, Louvain-la-Neuve 1348, Belgium

[§]Department of Physics, and Texas Center for Superconductivity, University of Houston, Houston, Texas 77204, United States

[∥]Center for Novel States of Complex Materials Research, Department of Physics and Astronomy, Seoul National University, Seoul 151-747, South Korea

Supporting Information

Successful implementations of many energy and transparent electronic applications, ranging from transparent conductors,[1] transparent complementary transistors,[2,3] high-power electronics,[4] to photovoltaics and solar fuel systems,[5−7] hinge on the discovery of a semiconductor with good carrier mobility and visible transparency. Transparent, *n*-type oxides such as ZnO, In−Sn−O, In−Ga−Zn−O, and others[8−11] have high electron mobility and are already in use in many devices. However, this stands in contrast to the *p*-type oxides, where the performances have not yet reached the same level as the *n*-type. This limitation is generally postulated to be as a result of the localization of the oxygen (O) 2p state in the valence band.[12,13] Driven by this realization, Hosono and co-workers have postulated the delocalization of the O 2p state as a strategy to unlock the high hole mobility, effectively decreasing the hole effective mass. They proposed an approach to accomplish this goal by incorporating highly electronegative cations with energy levels closely matched to the O 2p to increase the metal−oxygen hybridization.[14] This concept has led to the discovery of Cu-containing oxides[12,15] and oxysulfides[16−20] as high-performance wide-band gap, *p*-type materials. For visible-transparent, *p*-type oxides, the results from these Cu-systems are considered a hole mobility benchmark (∼1−10 $cm^2/(V{\cdot}s)$). Still, these values are modest when compared to the performances of the visible-transparent, *n*-type oxides (>100 $cm^2/(V{\cdot}s)$).[8,9,21] We note that Cu_2O can exhibit the hole mobility on the level of the *n*-type oxides.[22,23] However, Cu_2O is not transparent in the visible wavelength. For applications in transparent electronics and wide band gap transistors, the discovery of a new semiconducting oxide with high hole mobility and wide band gap is therefore an essential step forward.

In an effort to find superior *p*-type compounds, researchers have investigated the more spatially extended s-orbital chemistry to more efficiently delocalize the O 2p state.[24−27] Tin monoxide, SnO (Sn^{2+}: [Kr] $4d^{10}$ $5s^2$), has shown to be one of the most promising *p*-type s-orbital oxide candidates. However, SnO is still limited by the low hole mobility (<5 $cm^2/(V{\cdot}s)$), an anisotropic transport, and a low average transmission (75−80%).[25,26,28−30] Although recent report has shown the incorporation of metallic β-Sn can vastly improve the hole mobility (∼20 $cm^2/(V{\cdot}s)$),[31] preparing SnO with high stability is still a challenge. Bi^{3+} ([Xe] $4f^{14}$ $5d^{10}$ $6s^2$) compounds offers an alternative path to the s-orbital utilization.[27] However, the Bi 6s states in the studied Bi-based oxides thus far are too low for effective O 2p hybridization.[26] To take advantage of the s-orbital chemistry in Bi^{3+}, it is essential to find a structure and chemistry that has the Bi state at a suitable energy position to support the Bi 6s−O 2p hybridization while retaining visible transparency. We have recently reported the use of band gap and valence band curvatures as parameters for screening for high figure-of-merit *p*-type oxides from the binary and ternary oxide databases.[13] Herein, we report the experimental realization of an s-orbital bismuth-based candidate with strong metal−oxygen s−p hybridization and visible transparency. Our identification is a direct result of our application of the high-throughput computational screening methodology to the quaternary oxide space. We present its synthesis, optical and electrical characterization and provide a preliminary demonstration of the material's visible transparency and hole mobility to demonstrate the promising qualities of this *p*-type transparent oxide compound.

To identify our candidate, we searched among more than 3600 quaternary oxides present in the Materials Project database and originating from the Inorganic Crystal Structure Database (ICSD).[32,33] Our first step was to select materials with a low valence band effective mass in all crystallographic directions (<0.5 m_e) according to their density functional theory (DFT) band structures. Next, we computed the band gap of the most promising candidates using the GW method and finally evaluated the energy of the valence band maximum vs the vacuum level as an indicator of possible *p*-type character. This approach is similar to our previously published work.[13,34] The result from our screening is the identification of Ba_2BiTaO_6 (BBT, see Figure 1a) as a candidate for our *p*-type oxide study. BBT has a rhombohedral double-perovskite structure,[35−37] containing an ordered array of Bi^{3+} and Ta^{5+} ("B-site") octahedra surrounded by Ba^{2+} ("A-site"). The unique qualities of BBT are the low effective masses of its valence band (∼0.4−0.5 m_e, see Figure 1b), the high valence band maximum favoring *p*-type character (see the Supporting Information), and

Received: September 26, 2015
Revised: November 9, 2015
Published: December 8, 2015

DOI: 10.1021/acs.chemmater.5b03794
Chem. Mater. 2016, 28, 30−34

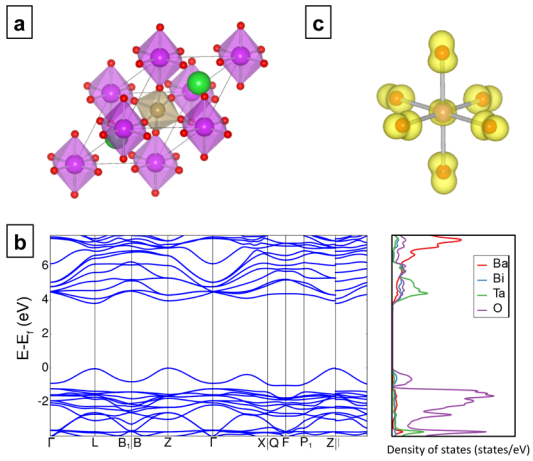

Figure 1. Crystal and electronic structure for Ba_2BiTaO_6. (a) Crystal structure of Ba_2BiTaO_6 in the rhombohedral space group ($R\bar{3}m$). (b) Band structure of Ba_2BiTaO_6 along symmetry lines and density of state projected on the different atomic sites using GGA. A scissor operator was applied to the band gap to make it fit the single-shot GW value. (c) Square of the wave function in DFT-GGA for the valence band in a BiO_6 octahedron.

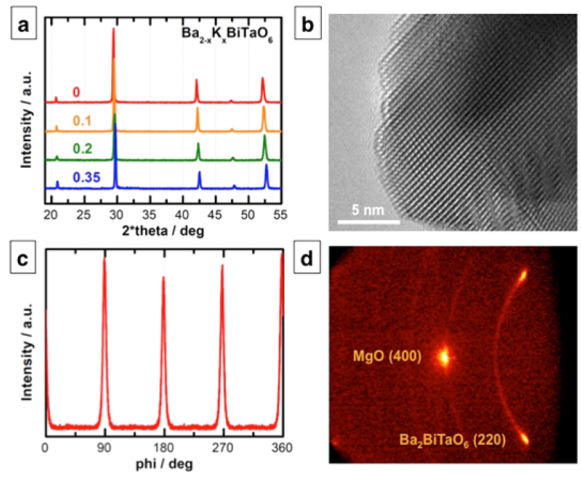

Figure 2. X-ray diffraction of the Ba_2BiTaO_6 powder and thin film. (a) Powder X-ray diffraction spectra for $Ba_{2-x}K_xBiTaO_6$. (b) TEM image of a Ba_2BiTaO_6 sample. (c) φ-Scan of the (220) peak of the Ba_2BiTaO_6 thin film. Both the GADDS and φ-scans suggest that our Ba_2BiTaO_6 as grown on MgO is texturized. (d) Bruker General Area Detector Diffraction System (GADDS) of the Ba_2BiTaO_6 thin film.

the visible-transparent band gap (calculated with GW to be around 3.8 eV). The first quality stems from the hybridization between the Bi 6s and the O 2p states as illustrated by the atomic projection of the valence band maximum (Figure 1c, see the Supporting Information for the bonding analysis). The charge density associated with the valence band shows that the Bi s-orbital hybridizes with the O 2p pointing toward the octahedron center while the two other perpendicular O 2p orbitals stay nonbonding (Figure 1c). The conduction band on the other hand is of a mixed Bi−Ta−O character and thereby shows less dispersion. The dominant Bi 6s−O 2p interaction in the valence band in BBT is similar to the $BaBiO_3$ perovskite, which has been extensively studied for its superconducting properties.[38−41] However, different from $BaBiO_3$, which has an optical gap around 2 eV,[42,43] BBT is transparent due to Ta^{5+} (which substitutes for Bi^{5+}). This inclusion pushes the conduction band upward and effectively increases the band gap. Interestingly, the electronic structure of BBT mimics what Sleight called the "Holy Grail" electronic structure for *p*-type oxide[27] with an s-based cationic state hybridizing with the oxygen 2p states. However, unlike other Bi-based oxides studied in the past, which generally have their Bi 6s state below the O 2p,[26,44] effectively limiting the Bi 6s−O 2p mixing, our chosen candidate has the Bi 6s level close the O 2p, which allows for a stronger Bi 6s−O 2p hybridization. We note that the finding of a compound with strong metal−oxygen hybridization and visible transparency was enabled by our ability to screen thousands of oxide compounds simultaneously; finding this unique structure−chemistry combination would have been more time-consuming by trials and errors.

To verify experimentally the prediction, we synthesize a phase-pure BBT using a solid-state synthesis. The phase purity was verified with X-ray diffraction (XRD, Figure 2a). All peaks match the double-perovskite rhombohedral structure of BBT that has been reported previously.[36,37] In the double-perovskite rhombohedral structure, Bi^{3+} and Ta^{5+} occupy distinct crystallographic positions; the observation of the rhombohedral structure therefore suggests that Bi and Ta do not form solid solution. Selected area diffraction using transmission electron microscopy (TEM) analysis confirms the rhombohedral assignment (see the Supporting Information) and a high-resolution TEM image confirms the crystallinity of the sample, in agreement with the XRD result (Figure 2b).

To evaluate the optical band gap, we conduct a transmission measurement on a BBT thin film using the BBT powder as a pulsed laser deposition (PLD) target for the thin film deposition. Using a single-crystal MgO (100) as a substrate for growth, we obtained a textured BBT film as verified by the XRD (Figure 2c,d) with a film thickness estimated to be ∼120 nm using spectroscopic ellipsometry. The textured microstructure is expected as a result of the in-plane compression of BBT (∼1.4% based on the pseudocubic lattice parameter of BBT). The optical transmittance of the BBT film had an average value of >90% in the wavelength range between 350 and 800 nm (Figure 3a). The direct optical band gap was

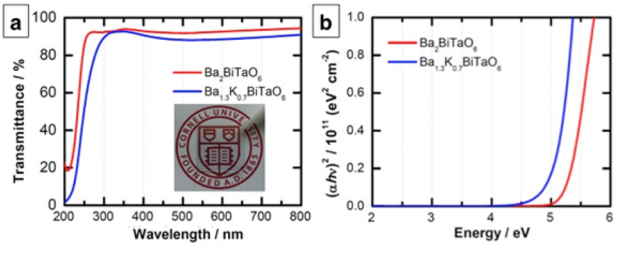

Figure 3. (a) Optical transmission and (b) $(\alpha h\upsilon)^2$ plot of the $Ba_{2-x}K_xBiTaO_6$ films grown on MgO(100) substrate. The film thickness is estimated around 120 nm.

estimated to be >4.5 eV (see Figure 3b). We note that this value is higher than the GW computed band gap. Optical absorption computations did not indicate that dipole forbidden transition could explain this discrepancy (see the Supporting Information) and we attribute it to an inherent underestimation from the single-shot GW approach.

Without extrinsic doping, BBT exhibited negligible conductivity in both the pellet and the thin film forms. We therefore examine the possibility of adding an electron acceptor to generate hole carriers. We elect to use K^+ for a Ba^{2+}

DOI: 10.1021/acs.chemmater.5b03794
Chem. Mater. 2016, 28, 30−34

aliovalent substitution, as K^+ has a similar ionic size as Ba^{2+}. We note that K^+ has previously been used to substitute Ba in $BaBiO_3$ for superconductivity.[38] Our XRD reveals that K^+ can be substituted up to 35% of Ba^{2+} in BBT (forming $Ba_{1.3}K_{0.7}BiTaO_6$, BKBT) without forming any noticeable secondary phase (Figure 2a). The K^+ substitution has small effects on the sample optical property; the PLD-deposited BKBT film shows that the visible transparency was largely preserved (>90%, Figure 3a). On the basis of this observation, we hypothesize that the K^+ inclusion did not lead to any optically active, midgap state formation. We point out that the optical band gap of our material decreases with K^+ concentration (Figure 3a,b). At the moment, the origin of this optical gap change is unclear; one possibility could be from the reduction in the lattice parameter following the K^+ substitution.

Having demonstrated the visible transparency of both BBT and BKBT, we now focus on evaluating the transport properties. Without K^+ incorporation, BBT exhibits no detectable conductivity, behaving as an intrinsic wide-band gap semiconductor. We therefore focus on the BKBT sample, specifically $Ba_{1.3}K_{0.7}BiTaO_6$, for the transport measurements. Our four-point probe measurements on the BKBT pellets reveal the conductivity in the range of ~ kΩ·cm. This level of conductivity precludes the possibility for a direct Hall measurement in thin-film geometry. We therefore elect to focus on a BKBT pellet, whose geometry affords a sufficient thickness to support the conductivity for the Hall experiment. The result from the Hall measurement (see the Supporting Information) shows that BKBT is a *p*-type material. We further extract the carrier concentration from the Hall experiment, which was found to be in the range of $\sim 10^{14}$ cm^{-3}. This is an astonishingly low carrier concentration given the amount of K^+ in the material; this level of carrier concentration has only been previously reported in high-quality single crystal works.[45−47] This suggests that our BKBT sample is strongly compensated by donor-like defects (e.g., oxygen vacancies). Overcoming this compensation will be an important step to bring BBT to its true potential and an experimental and theoretical study of BBT's defect behavior will be the subject of future work. We note that our difficulty in obtaining the *p*-type carrier even at high K^+ concentration is well-known in the bismuth oxide perovskites such as $Ba_{1-x}K_xBiO_3$, where the electron (*n*-type) conductivity still dominates even at 40% K substitution ($Ba_{0.58}K_{0.42}BiO_6$).[48,49]

We use the Hall carrier concentration from the BKBT pellet to estimate the hole mobility. We find that the value of μ_H to be in excess of 30 $cm^2/(V{\cdot}s)$. The observation of *p*-type conductivity is different from the transport data for $Ba_{0.58}K_{0.42}BiO_6$, which has *n*-type conductivity. In addition, the hole mobility in BKBT is higher than the electron mobility in $Ba_{0.58}K_{0.42}BiO_6$, which was found to be ~2 $cm^2/(V{\cdot}s)$,[48] likely as a result of the heavier electron in the bismuth perovskite system. Combining the mobility data with the optical gap, our BKBT compound represents the highest Hall hole mobility for a *p*-type transparent oxide with full range of visible transparency to our knowledge.

We point out that this preliminary value is likely an underestimation for BBT; we postulate that significantly higher hole mobility can be attained with a more dense, single-crystal BBT film. At the same time, we note that a realistic BBT-based device will need higher carrier concentration, which will likely cause scattering and lower the practical mobility. In any scenario, to utilize BBT for any practical application will require to increase carrier concentration by overcoming the likely defect compensation. Although it is difficult to predict if BKBT will be able to reach the carrier concentrations needed for "passive" transparent conducting oxides or if the mobility will still be high at the high carrier concentration, the exceptional transmission and mobility results justify a more careful attention to this promising material.

In summary, we have reported on a new chemistry of high-mobility, visibly transparent *p*-type oxide: Ba_2BiTaO_6. We identified this oxide using high-throughput computational screening. Experimental characterizations show Ba_2BiTaO_6 to have >90% high transmission in the visible and the highest reported *p*-type mobility for a transparent oxide. To our knowledge, this is the first reported transparent *p*-type compound that utilizes Bi 6s in its valence band, joining Bi^{3+} to the selected club of elements leading to *p*-type transparent oxides (such as Sn^{2+}, Cu^{1+} and Ag^{1+}). Although still limited by the carrier concentration, the exceptional performance of Ba_2BiTaO_6 is already evident in our preliminary characterizations. We further point out that Ba_2BiTaO_6 has a unique draw of having a ubiquitous perovskite structure, which offers a wide range of possibility of integrations with other functional perovskite materials.[50] Our work also shows how the "needle in a haystack problem" of materials discovery can be accelerated using high-throughput material computations, and how material informatics can help guide the experimental realization of new technological materials.

■ ASSOCIATED CONTENT

Supporting Information

The Supporting Information is available free of charge on the ACS Publications website at DOI: 10.1021/acs.chemmater.5b03794.

Experimental methods, valence band positions vs vacuum level, orbital overlap analysis, indirect optical transition, computed absorption coefficient for Ba_2BiTaO_6, Hall measurement on $Ba_{1.3}K_{0.7}BiTaO_6$ (PDF).

■ AUTHOR INFORMATION

Corresponding Authors

*Geoffroy Hautier. E-mail: geoffroy.hautier@uclouvain.be.
*Jin Suntivich. E-mail: jsuntivich@cornell.edu.

Author Contributions

⊥These authors contributed equally.

Notes

The authors declare no competing financial interest.

■ ACKNOWLEDGMENTS

The authors thank Dr. Christopher C. Evans and Chengyu Liu for their help with the ellipsometry, and Dr. Yuefeng Nie for help with the Hall measurement. G.H. and G.-M.R. acknowledge the F.R.S.-FNRS for financial support. The computational component of the work was supported by the European Union Marie Curie Career Integration (CIG) grant HTforTCOs PCIG11-GA-2012-321988. Computational resources have been provided by the supercomputing facilities of the Université catholique de Louvain (CISM/UCL) and the Consortium des Équipements de Calcul Intensif en Fédération Wallonie Bruxelles (CÉCI) funded by the Fond de la Recherche Scientifique de Belgique (F.R.S.-FNRS). H.J.K. and K.H.K. acknowledge financial supports from the National Creative

DOI: 10.1021/acs.chemmater.5b03794
Chem. Mater. 2016, 28, 30−34

Research Initiative (2010-0018300) through the NRF of Korea funded by the Ministry of Education, Science and Technology. The experimental part of the work made use of the Cornell Center for Materials Research Shared Facilities, which are supported through the NSF MRSEC program (DMR-1120296).

■ REFERENCES

(1) Ellmer, K. Past achievements and future challenges in the development of optically transparent electrodes. *Nat. Photonics* **2012**, *6*, 809−817.
(2) Kudo, A.; et al. Fabrication of transparent p-n heterojunction thin film diodes based entirely on oxide semiconductors. *Appl. Phys. Lett.* **1999**, *75*, 2851−2853.
(3) Ohta, H.; et al. Fabrication and photoresponse of a pn-heterojunction diode composed of transparent oxide semiconductors, p-NiO and n-ZnO. *Appl. Phys. Lett.* **2003**, *83*, 1029−1031.
(4) Morkoc, H.; et al. Large-band-gap SiC, III-V nitride, and II-VI ZnSe-based semiconductor device technologies. *J. Appl. Phys.* **1994**, *76*, 1363−1398.
(5) Stauber, R. E.; Perkins, J. D.; Parilla, P. A.; Ginley, D. S. Thin film growth of transparent p-type $CuAlO_2$. *Electrochem. Solid-State Lett.* **1999**, *2*, 654−656.
(6) Tonooka, K.; Bando, H.; Aiura, Y. Photovoltaic effect observed in transparent p-n heterojunctions based on oxide semiconductors. *Thin Solid Films* **2003**, *445*, 327−331.
(7) Izaki, M.; et al. Electrochemically constructed p-Cu_2O/n-ZnO heterojunction diode for photovoltaic device. *J. Phys. D: Appl. Phys.* **2007**, *40*, 3326−3329.
(8) Ohta, H.; et al. Highly electrically conductive indium-tin-oxide thin films epitaxially grown on yttria-stabilized zirconia (100) by pulsed-laser deposition. *Appl. Phys. Lett.* **2000**, *76*, 2740−2742.
(9) Look, D. C.; Droubay, T. C.; Chambers, S. A. Stable highly conductive ZnO via reduction of Zn vacancies. *Appl. Phys. Lett.* **2012**, *101*, 102101.
(10) Nomura, K.; et al. Room-temperature fabrication of transparent flexible thin-film transistors using amorphous oxide semiconductors. *Nature* **2004**, *432*, 488−492.
(11) Nomura, K.; et al. Thin-film transistor fabricated in single-crystalline transparent oxide semiconductor. *Science* **2003**, *300*, 1269−1272.
(12) Kawazoe, H.; Yanagi, H.; Ueda, K.; Hosono, H. Transparent p-type conducting oxides: Design and fabrication of p-n heterojunctions. *MRS Bull.* **2000**, *25*, 28−36.
(13) Hautier, G.; Miglio, A.; Ceder, G.; Rignanese, G. M.; Gonze, X. Identification and design principles of low hole effective mass p-type transparent conducting oxides. *Nat. Commun.* **2013**, *4*, 2292.
(14) Suntivich, J.; et al. Estimating Hybridization of Transition Metal and Oxygen States in Perovskites, from O K-edge X-ray Absorption Spectroscopy. *J. Phys. Chem. C* **2014**, *118*, 1856−1863.
(15) Kawazoe, H.; et al. P-type electrical conduction in transparent thin films of $CuAlO_2$. *Nature* **1997**, *389*, 939−942.
(16) Scanlon, D. O.; Buckeridge, J.; Catlow, C. R. A.; Watson, G. W. Understanding doping anomalies in degenerate p-type semiconductor LaCuOSe. *J. Mater. Chem. C* **2014**, *2*, 3429−3438.
(17) Ueda, K.; Inoue, S.; Hirose, S.; Kawazoe, H.; Hosono, H. Transparent p-type semiconductor: LaCuOS layered oxysulfide. *Appl. Phys. Lett.* **2000**, *77*, 2701−2703.
(18) Hiramatsu, H.; et al. Degenerate p-type conductivity in wide-gap $LaCuOS_{1-x}Se_x$ (x = 0 - 1) epitaxial films. *Appl. Phys. Lett.* **2003**, *82*, 1048−1050.
(19) Ueda, K.; Inoue, S.; Hosono, H.; Sarukura, N.; Hirano, M. Room-temperature excitons in wide-gap layered-oxysulfide semiconductor: LaCuOS. *Appl. Phys. Lett.* **2001**, *78*, 2333−2335.
(20) Scanlon, D. O.; Watson, G. W. (Cu_2S_2) $(Sr_3Sc_2O_5)$-A Layered, Direct Band Gap, p-Type Transparent Conducting Oxychalcogenide: A Theoretical Analysis. *Chem. Mater.* **2009**, *21*, 5435−5442.
(21) Carcia, P. F.; McLean, R. S.; Reilly, M. H.; Nunes, G. Transparent ZnO thin-film transistor fabricated by rf magnetron sputtering. *Appl. Phys. Lett.* **2003**, *82*, 1117−1119.
(22) Matsuzaki, K. Epitaxial growth of high mobility Cu_2O thin films and application to p-channel thin film transistor. *Appl. Phys. Lett.* **2008**, *93*, 202107.
(23) Fortin, E.; Weichman, F. L. Hall effect and electrical conductivity of Cu_2O monocrystals. *Can. J. Phys.* **1966**, *44*, 1551.
(24) Walsh, A.; Payne, D. J.; Egdell, R. G.; Watson, G. W. Stereochemistry of post-transition metal oxides: revision of the classical lone pair model. *Chem. Soc. Rev.* **2011**, *40*, 4455−4463.
(25) Ogo, Y.; et al. Tin monoxide as an s-orbital-based p-type oxide semiconductor: Electronic structures and TFT application. *Phys. Status Solidi A* **2009**, *206*, 2187−2191.
(26) Ogo, Y.; et al. p-channel thin-film transistor using p-type oxide semiconductor, SnO. *Appl. Phys. Lett.* **2008**, *93*, 032113.
(27) Sleight, A. In *Handbook of Transparent Conductors*; Ginley, D. S., Ed.; Springer: New York, 2011; pp 295−311.
(28) Fortunato, E. Transparent p-type SnO_x thin film transistors produced by reactive rf magnetron sputtering followed by low temperature annealing. *Appl. Phys. Lett.* **2010**, *97*, 052105.
(29) Quackenbush, N. F.; et al. Origin of the Bipolar Doping Behavior of SnO from X-ray Spectroscopy and Density Functional Theory. *Chem. Mater.* **2013**, *25*, 3114−3123.
(30) Allen, J. P.; Scanlon, D. O.; Piper, L. F. J.; Watson, G. W. Understanding the defect chemistry of tin monoxide. *J. Mater. Chem. C* **2013**, *1*, 8194−8208.
(31) Caraveo-Frescas, J. A.; et al. Record Mobility in Transparent p-Type Tin Monoxide Films and Devices by Phase Engineering. *ACS Nano* **2013**, *7*, 5160−5167.
(32) Jain, A.; et al. Commentary: The Materials Project: A materials genome approach to accelerating materials innovation. *APL Mater.* **2013**, *1*, 011002.
(33) Bergerhoff, G.; Hundt, R.; Sievers, R.; Brown, I. D. The Inorganic Crystal Structure Data Base. *J. Chem. Inf. Model.* **1983**, *23*, 66−69.
(34) Hautier, G.; Miglio, A.; Waroquiers, D.; Rignanese, G. M.; Gonze, X. How Does Chemistry Influence Electron Effective Mass in Oxides? A High-Throughput Computational Analysis. *Chem. Mater.* **2014**, *26*, 5447−5458.
(35) Wang, H.; et al. Synthesis, Structure, and Characterization of the Series $BaBi_{1-x}Ta_xO_3$ $(0 \le x \le 0.5)$. *Inorg. Chem.* **2010**, *49*, 5262−5270.
(36) Wallwork, K. S.; Kennedy, B. J.; Zhou, Q. D.; Lee, Y.; Vogt, T. Pressure and temperature-dependent structural studies of Ba_2BiTaO_6. *J. Solid State Chem.* **2005**, *178*, 207−211.
(37) Zhou, Q. D.; Kennedy, B. J. High temperature structural studies of Ba_2BiTaO_6. *Solid State Sci.* **2005**, *7*, 287−291.
(38) Baumert, B. A. Barium potassium bismuth oxide: A review. *J. Supercond.* **1995**, *8*, 175−181.
(39) Hinks, D. G.; et al. Synthesis, structure and superconductivity in the $Ba_{1-x}K_xBiO_{3-y}$ system. *Nature* **1988**, *333*, 836−838.
(40) Schneemeyer, L. F.; et al. Growth and structural characterization of superconducting $Ba_{1-x}K_xBiO_3$ single crystals. *Nature* **1988**, *335*, 421−423.
(41) Tseng, D.; Ruckenstein, E. Structure and superconductivity of $BaBiO_3$ doped with alkali ions. *J. Mater. Res.* **1990**, *5*, 742−745.
(42) Wang, Y. Y.; Feng, G. F.; Sutto, T. E.; Shao, Z. F. Dielectric function of $BaBiO_3$ investigated by electron-energy-loss spectroscopy and ellipsometry. *Phys. Rev. B: Condens. Matter Mater. Phys.* **1991**, *44*, 7098−7101.
(43) Federici, J. F.; Greene, B. I. Hartford, E. H., & Hellman, E. S., Optical characterization of excited states in $BaBiO_3$. *Phys. Rev. B: Condens. Matter Mater. Phys.* **1990**, *42*, 923−926.
(44) Hiramatsu, H.; et al. Crystal structures, optoelectronic properties, and electronic structures of layered oxychalcogenides MCuOCh (M = Bi, La; Ch = S, Se, Te): Effects of electronic configurations of M^{3+} ions. *Chem. Mater.* **2008**, *20*, 326−334.

DOI: 10.1021/acs.chemmater.5b03794
Chem. Mater. 2016, 28, 30−34

(45) Utsch, B.; Hausmann, A. Halleffekt und Leitfähigkeitsmessungen an Zinkoxid-Einkristallen mit Sauerstofflücken als Donatoren. *Z. Phys. B: Condens. Matter Quanta* **1975**, *21*, 27−31.
(46) Ellmer, K. Resistivity of polycrystalline zinc oxide films: current status and physical limit. *J. Phys. D: Appl. Phys.* **2001**, *34*, 3097−3108.
(47) Fleischer, M.; Meixner, H. Electron mobility in single-crystalline and polycrystalline Ga_2O_3. *J. Appl. Phys.* **1993**, *74*, 300−305.
(48) Minami, H.; Uwe, H. Electrical conductivity of the oxide superconductor $Ba_{0.58}K_{0.42}BiO_{2.96}$. *J. Phys. Soc. Jpn.* **1997**, *66*, 1771−1775.
(49) Lee, S. F.; et al. Hall effect and resistivity in metallic $Ba_{1-x}K_xBiO_3$ single crystals: Absence of 1/T dependence in R_h and linear-to-quadratic evolution of ρ(T)*. *Phys. C* **1993**, *209*, 141−144.
(50) Zhang, K. H. L.; et al. Perovskite Sr-Doped $LaCrO_3$ as a New p-Type Transparent Conducting Oxide. *Adv. Mater.* **2015**, *27*, 5191−5195.

DOI: 10.1021/acs.chemmater.5b03794
Chem. Mater. 2016, 28, 30−34